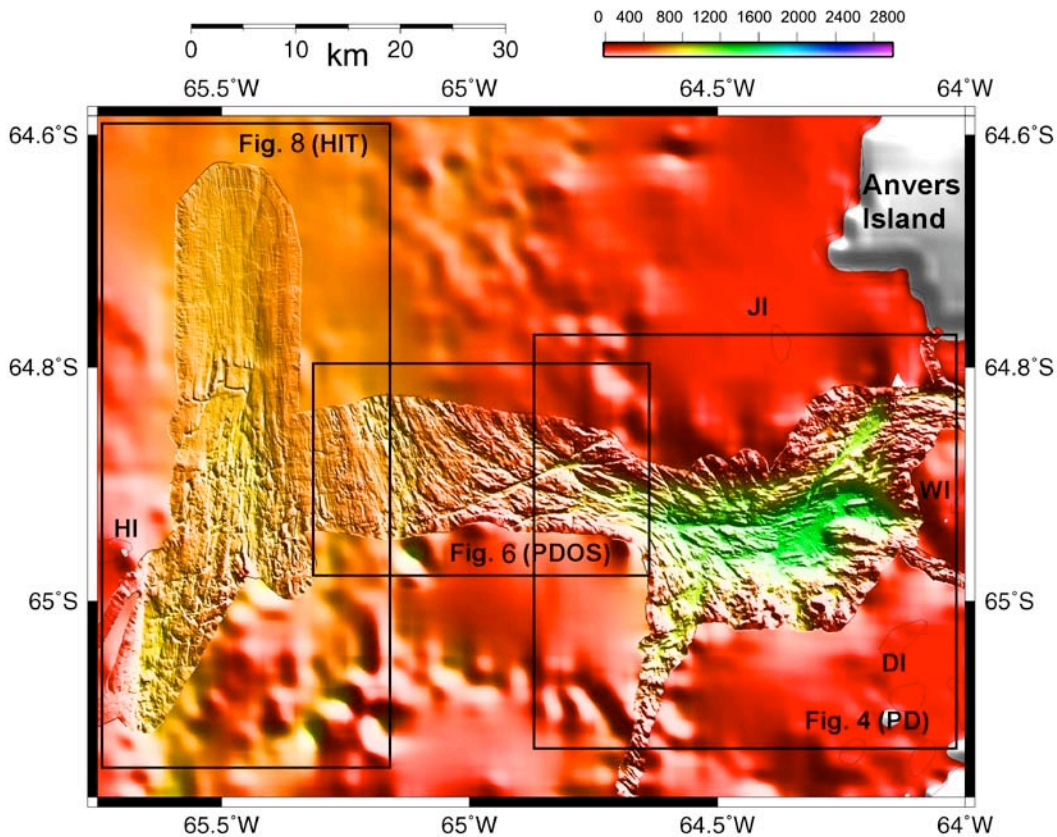


Subglacial Morphology and Glacial Evolution of the Palmer Deep Outlet System, Antarctic Peninsula

Eugene Domack^a,
David Amblàs^b, Robert Gilbert^c,
Stefanie Brachfeld^d
Angelo Camerlenghi^e, Michele Rebesco^e, Miquel Canals^b, and Roger Urgeles^b

- a. Department of Geology, Hamilton College, Clinton New York 13323, USA
- b. Department of Stratigraphy, Paleontology, and Marine Geosciences, University of Barcelona, 08028 Barcelona, Spain
- c. Department of Geography, Queen's University, Kingston Ontario K7L 3N6, Canada
- d. Earth & Environmental Studies, Montclair State University, Upper Montclair, New Jersey 07043, USA
- e. Istituto Nazionale di Oceanografia e di Geofisica Sperimentale, Trieste, Italy



Abstract

The Palmer Deep is an erosional, inner-shelf trough located at the convergence of ice flow from three distinct accumulation centers. It served as a funnel for ice flow out across the continental shelf of the Antarctic Peninsula. Swath mapping of 1440 km² of seafloor in and adjacent to the Palmer Deep basin defines a large paleo-ice stream that flowed 230 km across the Antarctic Peninsula continental shelf during the Last Glacial Maximum (MIS-2). The unique perspective and detail of the Palmer Deep physiography allow us to recognize several phases of erosion and deposition in the outlet basin. These events are uniquely constrained by two ODP drill cores (sites 1099 and 1098) that together recovered over 150 m of latest Pleistocene and Holocene sediment. We divide this region of the continental shelf into three zones based upon mega- to meso-scale bathymetric features and emphasize that all three were part of one glacial outlet during the most recent period of glaciation. These zones include from inner shelf to outer shelf: the Palmer Deep basin, the Palmer Deep Outlet Sill and the Hugo Island Trough. Specific seafloor features associated with these zones include: relict terraces, sub-glacial lake deltas, channels and levees, debris slopes, spindle and p-shaped bed forms, mega-scale glacial lineations, morainal banks, and bank breach points. The origin of many of these features can be linked to the development of a sub-glacial lake basin within the Palmer Deep during or prior to MIS-2, its subsequent drainage, and recession of the Palmer Deep ice stream system. It is significant to note that this sub-glacial lake system is reconstructed at the head of a major paleo-ice stream.

1. Introduction

The elongate and elevated terrain of the Antarctic Peninsula is surrounded by a relatively broad continental shelf that served as the platform for growth and expansion of an ice sheet during the Last Glacial Maximum (Payne et al., 1989; Anderson, 1999, Bentley and Anderson, 1998). A partition of the Antarctic Peninsula Ice Sheet into distinct ice stream systems is now known from regional swath mapping surveys that delineate distinct zones of accelerated flow, produced by the convergence of tributary glaciers. (Canals, et al., 2000, 2002, Camerlenghi, et al., 2001; Gilbert et al., 2003; O’Cofaigh et al., 2002, Lowe and Anderson, 2002; Amblas et al., 2005). Most of these ice streams received ice from bedrock valleys and fjords fed by ice accumulation along the spine of the Peninsula at elevations up to 2500 m. In contrast, the inner shelf of the Peninsula has been deeply scoured by glacial erosion; a process that has left deep troughs and basins that have served as depocenters for post-glacial marine sediment accumulation. The Palmer Deep (Fig. 1) is one of these erosional troughs located at the convergence of three distinct accumulation centers: Anvers Island, Flandres Bay, and the Graham Coast (Fig. 1). The Palmer Deep trough funneled ice flow out across the shelf where sub-glacial bed forms indicative of fast flow have been imaged (Fig. 2). A constricted sill lies in the transition between the clear ice stream portion of the mid to outer shelf and the Palmer Deep. Across this sill is a distinctive channelized morphology that reflects a combination of glacial melt water scour and underlying structural weakness within the bedrock (faulting and/or jointing).

We divide the sub-glacial landscape into three major zones based upon the meso- to mega-scale topography but emphasize that all three systems were part of one single

glacial outlet during the most recent period of expanded glaciation. These zones include from inner shelf to outer shelf:

- 1) the Palmer Deep basin (PD, Fig. 2)
- 2) the Palmer Deep Outlet Sill (PDOS, Fig. 2)
- 3) the Hugo Island Trough (HIT, Fig. 2).

Not discussed in this paper are the inner most feeder fjords that comprise the coastal portions of the drainage network and the main ice stream channel that made its way out across the continental shelf toward the shelf break (Fig. 1).

On a regional scale, based on low resolution, deep penetration multichannel seismic profiling, the nature of the substrate in the survey area likely consists of Mesozoic to Early Cenozoic volcanic and plutonic rocks (an acoustic basement of highly reflective seafloor with no signal penetration). In the northern part of Hugo Island Trough Zone a northward transition to the sedimentary substrate of the Mid-shelf basin, a Cenozoic sedimentary depo-center (interpreted either as fore arc or back arc basin) developed during the subduction history of the margin (Larter et al., 1997; Anderson, 1999).

2. Methods

Swath data were contributed by two cruises of the U. S. Antarctic Program (USAP) vessel *N.B. Palmer* (*NBP* 01-07 and *NBP* 99-03; Figs. 2 and 3) and one cruise of the Spanish R/V *Hesperides* (Fig. 1). Data were collected using a Seabeam 2100 multibeam echo sounder operated at 12 kHz (*N.B. Palmer*) and a Simrad EM12S swath-bathymetry system (*R/V Hesperides*). Post collection processing included editing of individual ping traces with quality control supervised and documented by Antarctic Support Associates, Raytheon Polar Services, and the geophysical staff at the University of Barcelona. USAP data are archived at Lamont-Doherty Geological Observatory (<http://data.ldeo.columbia.edu/antarctic>). In addition, coarse scale bathymetry was derived from the GEOSAT sea surface altimetry (Smith and Sandwell, 1997) and stitched to areas of the seafloor surrounding the available swath data (Fig. 1). Seismic reflection data were collected using a variety of systems from HUNTEC deep towed boomer to single channel, towed Generator Injector gun (Fig. AF1., in Barker et al., 1999).

Two Ocean Drilling Program (ODP) sites were occupied within the Palmer Deep during Leg 178, sites 1098 and 1099 (Fig. 3; Barker and Camerlenghi, 2002; Barker et al., 1999). A third, jumbo piston core was collected during cruise *NBP*99-03 (Domack et al., 2003). In addition, gravity (kasten) cores were collected at all sites in order to provide calibration and correlation to the sediment water interface for subsequent radiocarbon analyses of down-core material.

Radiocarbon analyses (via AMS) were conducted on foraminifera, mollusc, and total organic matter fractions as discussed previously (see, Domack et al., 2001; Domack et al., 2003). We include 25 previously unpublished dates in this paper (Table 1) from Site 1099 and associated gravity core KC-26.

3. Observations of Seafloor Bathymetry

3.1. Palmer Deep

Within the Palmer Deep (PD; Fig. 2) we recognize both depositional and erosional features that are related to the glacial and post-glacial history of the basin. The bedrock surrounding the PD is crystalline metamorphic and igneous rock related to Cenozoic arc volcanism. These rocks were uplifted and dissected by extensive glaciation that commenced in the Miocene (Barker and Camerlenghi., 2002). The large-scale morphology of the Palmer Deep basin is dominated by streamlined bedrock sculpted by glacial abrasion and plucking. Zones of structural weakness within the crystalline basement (joints and faults) are accentuated by the glacial erosion, with most of these features oriented obliquely at 65° and 120° (Rebesco et al., 1998; Sniffen, 2001). Glacial flow patterns can readily be inferred to have paralleled the east-west elongation of the Palmer Deep basin with inflow from the surrounding elevated terrain of Anvers Island, along Bismark Strait, and Graham Land (Fig. 2).

However, superimposed upon this overall streamlined relief are mega- to mesoscale features that are revealed by detailed contouring of swath bathymetry (Fig. 3). Based upon the relief depicted in Fig. 3 we recognize distinctive submarine features including: slope terraces, basin floor, channels, and prograded slopes (Fig. 4).

The eastern end of the PD is characterized by a steep, smooth slope (22°) with a relief of 1200 m. Seismic reflection profiles across this slope indicate an internal set of prograded reflectors originating as debris flows (Fig. 5; Rebesco et al., 1998). This depositional slope has undergone little apparent degradation or glacial erosion. Its steep relief indicates significant slope stability as would be likely if it were cored by cohesive, poorly sorted deposits such as diamicton. Unlike the eastern end of the PD, the northern and southern slopes are punctuated by distinctive terraces or perched basins that lie primarily between 500 and 900 m in depth. These terraces range in size from several hundred m² to 4 km² with relief of less than 20 m. At least 25 terraces are recognized along the northern and southern PD slopes (Fig. 4).

The western end of the PD has both depositional and erosional features and is characterized by a roughly triangular area of flat relief (16 km²) that breaks eastward into a smooth slope of 0° to 3.4°, interpreted as a relict delta. In support of this interpretation there are seismic profiles such as BAS line 845-03, S.P. 100-150 (Rob Larter, unpublished), OGS profile IT95-H220 -H221 (Rebesco et al., 1998), and USAP deep-tow Hunttech profile *LMG* 98-2 (Domack, unpublished) that indicate sub-bottom reflectivity in this area (generated by soft sediments of a submarine delta) as opposed to the high amplitude and seafloor reflection, with no energy penetration, typical of the northern and southern sides of the PD basin cast in hard rock or covered by diamict. The western slope of the PD is therefore much gentler than the steeper eastern slope (Fig. 3). The western slope of the basin is also dissected by a series of tributary channels (Fig. 4). These merge eastward and deepen into a single incised channel, up to 200 m wide and 50-100 m deep that extends 24 km, in a roughly west to east direction. This channel terminates in the flat basin floor of the PD, at a depth of 1400 m, but not before it takes a sharp southerly turn. The longitudinal profile of the PD channel is continuous and unbroken by reversals in slope, consistent with an origin related to sediment gravity flows. Levees (20-40 m high) parallel the channel in portions of the PD basin deeper than 1300 m (Fig. 3).

The basin floor of the PD generally lies below 1200 m depth; here there is only the slightest indication of glacial sculpting, characteristic of the shallow basement rocks

that surround the PD. At 1400 m depth the basin floor is flat and the seismic profiles show ponded sediments in excess of 200 m thick (Rebesco et al., 1998; Kirby et al., 1998). Ocean Drilling Program (ODP) Site 1099 was located in these ponded sediments (Barker et al., 1999) and recovered 108 m of unconsolidated sediment before drilling was terminated due to time constraints.

3.2. *Palmer Deep Outlet Sill*

Toward the west the PD basin transitions into a shallow silled region of 420 km² that is characterized by a distinctive channelized terrain (Fig. 6). We refer to this region as the PD Outlet Sill (PDOS) as the glacially streamlined topography clearly indicates ice flow out of the PD basin, onto the continental shelf, via this constricted topography (Fig. 2).

The channels of the PDOS are broad (200 - 500 m wide), deep (100 - 300 m), and intersect at distinct 75° to 50° angles (Figs. 6 and 7). This later characteristic reflects an underlying structural control, with faulting or joint sets striking 65° to 140° azimuth (Hawkes, 1981). Yet the NW to SE oriented channels conform to the overall glacial streamlining of the seafloor by taking on a curvilinear pattern toward the open shelf (Fig. 2). Intersection points are typically over-deepened, and individual channels demonstrate ubiquitous reversals in longitudinal profile. Channel sides vary in relief with some very steep slopes (45° or more) and some more gentle. Where the channels are over deepened and broad, the cross-section is typically U-shaped, whereas more narrow interconnecting channels are typically V-shaped (Fig. 6). The extent to which this reflects deposition or strictly erosion is irresolvable with current imaging techniques. However, all of the observed characteristics of the PDOS channels are similar to “anastomosing channels” previously described from the Pine Island Bay trough, Antarctic Peninsula (Lowe and Anderson, 2002) and are of the same scale as The Labyrinth channels found at the head of Taylor Valley in the Dry Valleys of Victoria Land (Benn and Evans, 1998) and the Gwaun-Jordonston drainage networks of Wales (Sugden and John, 1976). The inter-channel areas of the PDOS demonstrate a glacially streamlined relief similar to the crystalline basement that surrounds the PD basin proper (Fig. 3). However, there appear to be more distinctive drumlin-like bed forms (Fig. 6) with steep stoss noses and elongate lee tails, rather than the more uniform erosional sculpting (areal scouring) typical of the crystalline basement rocks surrounding the PD. These former features are similar to “roches moutonnées” described from the adjacent Biscoe Trough (see Fig. 2a. in Canals et al., 2003, p. 102). However, the quarried lee side terminations, typical of classic roches moutonnées, are not resolved by available imagery techniques.

Toward the west the broad series of channels end by opening into a series of dispersed and shallow incisions that trend west to northwest (Fig. 7). These distributary features occur where the relief decreases and progressively deepens to between 500 and 800 m (Fig. 6). In a gradual fashion the integrity of the channels is lost toward the open continental shelf but the overall streamlining of the seafloor is still preserved (Fig. 2) by increasingly elongate bed forms.

3.3. *Hugo Island Trough*

The PDOS merges with a second ice drainage system just east of Hugo Island (Figs. 1 and 2). Here the flow patterns are clearly delineated by a streamlined topography

referred to as the Hugo Island Trough (HIT; Fig. 8). The HIT maintains its integrity out across the continental shelf until it merges with yet another drainage outlet just northwest of Anvers Island (Fig. 1). This combined system exits the continental shelf 150 km northwest of the PD basin. Within the HIT the seafloor morphology changes into a lineated one, dominated by mega-scale glacial lineations (Figs. 8 and 9). Such transition reflects the change from crystalline bedrock to the Mid-shelf Basin sedimentary substratum. Similar morphological changes induced by changing basement have been observed elsewhere along the Antarctic margin (Anderson et al., 2001; Camerlenghi et al., 2001; O’Cofaigh et al., 2002).

The mega-scale glacial lineations are more evident just northward (in a seaward direction) of a prominent set of scarps that mark either a (depositional) grounding line wedge or (bedrock) submarine cuesta (Fig. 9). The scarps also delineate the seaward limit of a rough seafloor morphology characterized by relatively small but high relief incisions (channels) that converge toward a break in the scarp (Figs. 8 and 9). The morphology landward of the break is negative, while seaward of the scarp the breach point is of positive relief. This association is similar to that of forms marking the breach in submarine moraines from the Mertz Trough, off the East Antarctic margin (McMullen et al., 2002).

The mega scale glacial lineations within the HIT run due north for at least 30 km (Fig. 9) and likely extend to the shelf break another 120 km, where sub glacial grounding line features have been imaged (Larter and Vanneste, 1995). Unlike the shallow outer shelf of most of the Antarctic margin (Shipp et al., 1999) there is little evidence of iceberg scour across these features in the HIT. The scale of the lineations (~ 25 m high, 2 km in wavelength) is identical to features recognized from the Ross Sea (Shipp et al., 1999; 2002) and Mertz Trough (McMullen et al., 2002). There is no evidence of channels within the mega-scale glacial lineations, so characteristic of the PD basin and PDOS system.

4. Sediment Core Stratigraphy

The chronology we present (table 1 and Fig. 10) is based upon accelerator ¹⁴C dating of marine organic matter (25 samples) and correlation of physical properties to a calibrated radiocarbon time scale from the immediate vicinity of site 1099. We note that there are difficulties in the application of radiocarbon dating to marine sediments in Antarctica due to the large reservoir effect (Harden et al., 1992; Björck et al., 1991; Gordon and Harkness, 1992) and corrections for reworked organic particulates (Domack et al., 1999; Andrews, et al., 1999). Yet the Palmer Deep record is exceptional in that surface organic matter provides radiocarbon ages equal to established reservoir ages (Site 1098) and the correction for reworking of detrital organic matter is minimal (360 years) at site 1099 (Fig. 10, table 1). Replicate analyses also provide excellent agreement that is less than the laboratory (analytical) error of ± 50 years. Hence the Palmer Deep sedimentary record contains a very reliable radiocarbon chronology and serves as a circum Antarctic paleoenvironmental reference section (Domack et al., 2001).

At site 1099, 108 m of interbedded laminated diatom ooze/sandy mud and homogenous diatom mud/thin muddy sand (Fig. 10) record alternating periods of hemipelagic and ice rafted deposition interrupted by periodic turbidity current deposition,

including one megaturbidite. Rates of hemipelagic sedimentation are 2 to 7 mm/yr. The large-scale turbidite sequences are consistent with site 1099 being located on the flat basin floor of the Palmer Deep (Kirby et al., 1998). We divide the stratigraphy into four units consistent with previous division of the nearby site 1098 lithofacies. Unit I is late Holocene in age (0 to 3250 cal. yr BP) and consists of interbedded diatom mud turbidites and hemipelagic diatom mud that accumulated at rates of less than 1 mm/yr (exclusive of turbidites; Kirby et al., 1998). Unit I is characterized by relatively high and variable magnetic susceptibility, reflecting a dominance of small multidomain magnetite and interbedding of diatom-rich (paramagnetic) and diatom poor laminations. Unit II consists of laminated diatom mud and ooze with fewer and thinner diatom mud turbidites that accumulated at rates of up to 3.2 mm/yr. It is characterized by lower magnetic susceptibility and ranges in age from 3.2 ka to 8.0 yr BP. Units I and II represent the late Holocene Neoglaciation and the middle Holocene climatic optimum, respectively. These units can be unambiguously correlated by age, sedimentary structures, and MS with site 1098 (Figs. 3 and 10), thus attesting to the robust application of corrected radiocarbon ages in both sequences. Unit III is characterized by unusually thick turbidite intervals, one in excess of 30 m that are interbedded with laminated diatom ooze and mud and contain concentrations of ice rafted debris (IRD). In places, such IRD comprises a thin bed where concentrations of ice-rafted material were sufficient to produce a poorly sorted diamicton (Fig. 10). Unlike all other turbidites in core 1099AB, the megaturbidite (MT-2 at 35 to 75 m below the sediment surface; Fig. 10) is marked by coarse, gravelly sand at its base, clearly attesting to the energy of transport within the Palmer Deep basin at that time. Unit III dates to between 8 ka to 11.5 ka yr BP.

The bottom sediments (Unit IV) in cores from Site 1099B are rhythmically laminated diatom ooze and sandy mud. These laminations are varves that record unique conditions during the recession of glacial ice from within the PD basin (Leventer et al., 2002). These varved sediments likely extend beyond the 108 m reach of Site 1098 and are underlain by an additional 100 m of unconsolidated sediment, most likely with additional turbidite intervals (Barker et al., 2001). The varved sediments at Site 1099 date to between 12,600 and 11,800 BP. Hence, the total thickness of basin fill (~200 m) and its character within the PD have yet to be recovered by drilling or coring.

The entire sediment package to basement was recovered at site 1098 located in a perched basin in water depths of 1000 m, some 12 km to the northeast of Site 1099 (Fig. 3). The recovered stratigraphy is identical to that from 1099 except for the exclusion of thick turbidites (Domack et al., 2001). At Site 1098, 45 m of post-glacial sediment was found to overly glacial diamicton (till) consistent with the seismic stratigraphy of the site (Rebesco et al., 1998; Barker et al., 2001). Details of the sediments at Site 1098 are summarized by Domack (2002).

5. Interpretation

There is little doubt that the continental shelf surrounding the Palmer Deep has undergone many episodes of late Neogene to Quaternary glaciation (Barker et al. 1999; Bart and Anderson, 1995; Larter et al., 1997). The present seafloor relief must therefore reflect repeated modification, if not amplification, by these multiple glaciations. Yet seismic reflection data (Rebesco et al., 1998, Barker et al., 1999), the established sediment core stratigraphy (Kirby et al., 1998; Domack et al., 2001; 2003), and terrestrial

records (Hjort et al., 2003) clearly constrain the most recent episode of glacial erosion and glacial marine deposition during and following the Last Glacial Maximum. Within this time frame, Marine Isotope Stage 2 (LGM, MIS-2) we therefore propose several stages in the evolution of the basin as discussed below.

5.1. Ice Dome Growth and Expansion

A phase of expanding glaciation coincided with period(s) of lowered eustatic sea level, ice dome growth (flow divergence), and flow convergence into the PD. Today there remain two elevated ice domes greater than 2000 m above sea level, one on Anvers Island (The Maar Ice Piedmont) and the other the glacial carapace of the Bruce Plateau, Graham Land (Figs. 1 and 11). It is important to note that both of these ice domes are immediately adjacent to the northern and southern margins of the PD basin via shallow coastal waters (less than 200 m; Fig. 2). These shallows extend around the PD basin to within 2 km, as marked by the emergence of the Joubin, Wauwermans, Dannebrog, Myriad, and Argentine Islands, collectively known as the Wilhelm Archipelago (Figs. 2 and 3). Today, all of these islands are mantled by thin ice/firn caps whose extents are only limited by the small size of the emergent rock and wave action along the shore (Fig 11b). During periods of lowered sea level, such as the transition from MIS-3 to MIS-2 or earlier, the extent of emergent land would have increased, and seaward expansion of the Anvers Island and Bruce Plateau ice domes could have quickly encroached upon the northern and southern rim of the PD basin. Likewise, the Hugo Island, Betbeder and Pitt Island system to the west to southwest (respectively) would have also provided emergent platforms for the formation of localized ice caps. This, coupled with colder temperatures, would have provided the impetus (pinning points) for the formation of localized ice shelf conditions within, or across, the PD basin. At this time a glacial flow directed from east to west through the PD Basin was fed by way of the Bismark Strait and its tributaries, the Neumayer Channel and Flandres Bay. The outlet glaciers that drained the southeastern slopes of Anvers Island and the northern edge of the Bruce Plateau, progressively expanded their grounding lines through the depth (greater than 800 m) and length (30 to 50 km) of the Neumayer Channel and Etienne Fjord/ Flandres Bay, respectively.

5.2. Sub-Glacial Lake in Palmer Deep basin

The presence of a sub-glacial lake within the Palmer Deep was first proposed by Rebesco et al., (1998) and critical in the argument for its formation is the requirement of near complete encirclement by grounded glacial ice around the basin. We believe that this was quite plausible given the above discussion. The evidence for the lake basin itself is partially preserved in the form of depositional slopes around the PD basin (Fig 4). The western end of the basin we believe is the erosional remnant of a sub-glacial lake delta that at one time was fed by sub-glacial melt water emanating from the channels of the PDOS (Figs. 2-4). The use of the term sub-glacial lake delta follows the usage of the term by Gjessing (1960) and subsequently discussed and illustrated by Sugden and John (1976). In this use of the term, and of the feature recognized in the PD, the sub-glacial lake delta sediments do not record a local or global base level, as terrestrial deltas do. Instead, they record the upward transition of sediments into a standing body of water in accordance to this change in hydraulic conditions. Flow into a confined water body

beneath glacial ice implies some loss of volume of the reservoir (under melting of ice) which is compensated by fluid flow into the system. Hence the velocity and consequent turbulence of the melt water inflow into the lake would be limited, unless there was a free water surface connection to the atmosphere.

A conservative estimate of the volume of the PD sub-glacial lake is about 20 km³ and its greatest depth would have been on the order of 800 m, if the terraces and delta mark the ice-water interface and the deep basin fill (200 m of sediment) is removed. Its surface dimension, although somewhat irregular, would have been approximately 8 km in diameter. This is small compared to known Antarctic sub-glacial lakes whose dimensions are estimated by widely spaced radio echo sounding (Siegert et al., 1996). Modern Antarctic sub-glacial lakes all lay beneath 2.3 km or more of ice, are found along major ice divides (low surface gradient and ice velocity), and are 300 km or more from the coast (Siegert et al., 1996). However, the relief of the PD sub-glacial lake is much better known than any existing sub-glacial lake basin, including sub-glacial Lake Vostok (Kapista et al., 1996). It is important to note that hydraulic pressure feeding into the delta system (via the PDSO channels) was in excess of the cryostatic force of the ice shelf across the PD basin. This could result if localized domes southwest of the PD basin at the time where significantly thick and/or significant melt water production from the surface plumbed (i.e. Zwally et al., 2002) the PDOS channel system. At this stage in the development of the system we require a reversal in ice surface slope from the normal down gradient decrease in elevation. This is consistent with both the observed ice surface character over existing sub-glacial lakes (such as at Vostok, Kapista et al., 1996) and a newly proposed model for sub-glacial lake formation during glacial expansion across continental shelves (Alley et al., this volume). Critical to the later model is the requirement for at least partial marine salinity of entrapped water during lake formation, which helps to prevent large scale freezing of the reservoir beneath glacial ice.

The prograding slopes of the delta, that should contain foresets, are only partially preserved along the southern and northern edge of the basin as low relief, relatively low angle depositional slopes. These were dissected by subsequent gravity flows in the middle (Figs. 3 and 4). Therefore, the former delta predates the PD turbidite channel since it is cross-cut (eroded) by the channel tributaries. The gentle foreset slope of the delta likely represents fine-grained sediment of silt or mud, rather than coarse and cohesive diamicton that would be expected to have a higher angle of repose such as found along the eastern end of the PD basin.

In the late stage of the Palmer Deep sub-glacial lake, ice flowing out of the Bismarck Strait is likely to have created a grounding line as it encroached from the east. The flow of the outlet system at this end of the basin was responsible for progradation of a debris slope (resulting from the accumulation of debris flows) and the development of the steep and even relief along the eastern end of the basin (Figs. 3 and 4). This steep prograded slope clearly predates the deep basin fill strata which pond and on-lap near-surface reflectors that comprise the slope (Rebesco et al., 1998; Fig. 5).

The terraces identified along the northern and southern slopes of the PD basin (Fig. 4) are interpreted to represent the ponding of fine sediment within depressions or breaks in the slope. The fine detritus originated as dilute melt plumes which emanated from along the grounding line/ shoreline of the sub-glacial lake. Such processes are observed today from within fjord heads where dilute glacial melt waters transport silt and

clay aggregates (flocs) out from underneath sub-glacial cavities (Domack and Williams, 1990; Domack et al., 1994). Coring of one of the terraces in the PD (JPC 10; Fig. 3) recovered 12 m of post-glacial marine diatom ooze overlying clay and laminated diatom bearing mud, dated to 9000 yr BP (Domack et al., 2003). No diamict was recovered at this site.

5.3. Shelf Edge Grounding and Evacuation of Palmer Deep sub-glacial lake

Eventually with continued low sea level conditions and build up of ice along the elevated domes glacial expansion forced ice to ground within the PD basin and merge with tributaries out across the PDOS, HIT, and continental shelf. The mega-scale glacial lineations and drumlinized seafloor of the outer PDOS and HIT are evidence of this. The glacial sculpting along the flanks and bottom of the PD basin also took place at this time. Yet these later features are partially buried by post-glacial marine sediment in the PD basin. Partial erosion of the delta also took place at this time, perhaps focused by faster flow in the central portion of the PD basin. As ice thickened and surface elevations became steeper, water within the PD sub-glacial lake must have been forced to drain to the west down the hydrostatic gradient. This gradient would have been partially reversed from earlier on and would have forced water out through the PDOS channels (Fig. 7), thus further eroding and reshaping them. This would have occurred at a time of maximum ice extent and thickness and is consistent with new models for sub-glacial lake formation along glaciated continental shelves during maximum glaciations (Alley et al., this volume).

Maximum ice thickness is envisaged to have produced distinct domes larger than those on Anvers Island (Palmer Archipelago) and along the Graham Land Coast (Fig. 12). The Graham Land dome is proposed to have occupied the region just east of the PD basin where erosional landforms (horns) indicative of radial flow are prominent features of the coastal landscape (Fig. 11c; see also Fig. 9.1 in Skinner et al., 1999, p. 190)

The flushing of basal water out through the PDOS into the HIT could have helped lubricate the bed and hence sculpt glacial till. The bed forms leading out of the PDOS channels indicate dispersal of melt water not confinement (Fig. 4). Hence, one mechanism of enhancing glacial flow out through the PD ice stream system could have been provided by closure of the PD basin sub-glacial lake. We suggest that this enhanced the development of mega-scale glacial lineations within the main axis of flow by increasing the flow velocity across and within the substrate. The volume of water within the PD sub-glacial lake was unlikely sufficient to provide a through flow to the shelf edge but enhanced ice flow in the inner most part of the shelf could have provided one way to lower the ice elevation across the inner shelf at the same time as eustatic sea levels were beginning to rise.

5.4. Lowering of glacial surface and recession of ice stream system

We hypothesize that with the addition of basal water to the till system beneath the outer HIT, flow of the PD outlet accelerated. This could have been aided by addition of surface melt water if climate conditions warmed following the LGM (MIS-2) as surface melt water today accelerates flow of the Greenland Ice Sheet and its outlets (Zwally, et al., 2002). With acceleration of drainage, via the PD ice stream, surface elevations of the

surrounding ice sheet would have decreased, leading eventually to thinner ice within the ice stream and its drainage. Such a lowering of ice surface elevations following maximum conditions, when coupled with rising eustatic sea levels, would have provided sufficient instability to increase calving rates. Hence, we envision a situation where calving bay reentrants (see Hillefors, 1979) were created along the entire front of the PD ice stream during deglaciation. As the ice stream system retreated across the PD basin, restricted conditions of circulation and enhanced sediment focusing within the PD basin commenced, consistent with the detailed stratigraphy of ODP sites 1098 and 1099 (Leventer et al., 2002). In cores from Site 1098, at the bottom of the section above glacial till there is a unique varved sequence of diatom ooze and sandy, silty, clay. This lithofacies represents very high productivity and deposition of ice-rafted material in annual cycles for a period of approximately 200 years. The identical interval is found in Site 1099, although the contact with glacial till was not recovered (Fig. 10).

5.5. Dissection of relict delta and turbidite channels in Palmer Deep basin

As the PD basin became a marine system it is clear that significant erosion of the relict delta at the western end led to incision of the major channels leading down into the PD basin floor (Fig. 4). The products of this instability and erosion were numerous as evidenced by the massive turbidites ponded in the deep basin. At Site 1099 (Fig. 10) one of these turbidites is 30 m thick and comprises what is termed a megaturbidite (Bouma, 1987; Rebesco et al., 2000). These were deposited as recently as 9000 yr BP, while most were deposited prior to this as shown by another 100 m of section lying below the cored intervals at Site 1099. The seismic reflection data from across the PD basin clearly indicate that the basin infill post-dates the debris slope of the eastern end of the basin (Rebesco et al., 1998; Fig. 5). In addition, the subtle glacial sculpting of the PD basin itself, a product of maximum glacial conditions, is partially masked by the turbidite infill at the bottom of the basin. Following this initial period of sediment gravity flows, hemipelagic and pelagic deposition dominated across the PD basin with slightly more recent deglaciation within the perched basin at Site 1098 (Fig. 3).

5.6. Clearance of glacial ice from the Bismark and Gerlache Strait and Neumayer Channel

The final episode in deglaciation was the clearance of the straits between Anvers Island and the Danco Coast, a section of the Graham Land Coast. This was accomplished by 8000 yr BP as post glacial marine sediments within the fjords date to 7000 to 8000 yr BP (Ingólfsson and Hjort, 2002; Shevenell et al., 1996; unpublished data from Paradise Harbor). We suggest that this final phase of retreat from the trough began with the calving bay reentrants across the continental shelf. Accompanying this was recession of ice from the shallow banks surrounding Anvers Island and the Wilhelm Archipelago coincident with final phases of eustatic sea level rise.

6. Conclusions

Detailed bathymetric characteristics and seafloor relief coupled with stratigraphic observations from ODP Sites 1098 and 1099 support the occurrence of a sub-glacial lake within the PD basin just prior to the LGM (MIS-2) conditions. We propose the following sequence of events to explain the specific morphologic features and stratigraphic units associated with the Palmer Deep ice stream system.

- 1) A Phase of initial glaciation coincided with period(s) of lowered eustatic sea level, ice dome growth (expansion and flow divergence), and flow convergence into PD.
- 2) A phase of sub-glacial lake formation was induced by ice shelf cover over the Palmer Deep and grounding across the PDOS. This phase was associated with initiation of back flow of ice and some sub glacial melt water into the basin. Formation of PD slope features occurred such as the delta on the western slope, the steep debris flow slope, and terraces along the northern and southern margins. The delta was fed by sub glacial melt water that converged toward the east, via the early stage melt water channels of the PDOS system.
- 3) Glacial expansion and grounding of glacial ice within the PD basin and to the shelf edge occurred during the period of lowest sea level (MIS-2) about 22 to 18 ka BP. Glacial abrasion within the PD basin, PDOS, and HIT initiated the formation of mega-scale glacial lineations.
- 4) Melt water evacuated the PD sub glacial lake via the PDOS and HIT as it enlarged the sub-glacial melt water channels in the PDOS system, breached scarps within the HIT and dispersed melt water into the HIT and till substrate. This was associated with enhanced streaming of ice through the entire outlet system but especially with the HIT.
- 5) This melt water evacuation enhanced the flow of the ice stream, which subsequently lowered the ice surface.
- 6) Calving bay reentrants caused recession of the ice stream progressively back into the PD basin from the outer to middle shelf, to the HIT and the PDOS systems.
- 7) The delta in the western end of the PD basin was dissected and a turbidite channel in the PD basin was created by sediment gravity flows which also deposited the ponded sequence recovered from ODP Site 1099 commencing about 13,000 yr BP.
- 8) A pelagic and hemipelagic sediment drape formed across the terraces and Palmer Deep basins since ~11,000 yr BP (ODP Site 1098, 1099, and Jumbo Piston Core site 10).
- 9) Glacial ice left the straits between Anvers Island and the Graham Land Coast (Fig. 1) and retreated to fjord headlands by around 7 to 8 ka y BP.

The characteristics of the PD sub-glacial lake may have important analogies with existing sub-glacial lakes beneath the Antarctic Ice Sheet (Oswald and Robin, 1973; Kapista, et al., 1996; Siegert et al., 1996), former ice sheets (Shoemaker, 1991) and the drainage of former ice sheets and their sub glacial reservoirs of water (Shoemaker, 1991; Alley, et al., this volume). The timing of events is also significant and our results indicate deglaciation of the PD basin by 13 ka, some 1 ka after Meltwater Pulse 1A, suggested by

some to have been caused by Antarctic glacial recession (Clark et al., 2002). Yet the PD results are in-phase with the timing for glacial recession in the western Ross Sea (Domack et al., 1999), the NW Weddell Sea (Brachfeld et al., 2003), and the Prydz Bay continental shelf (Domack et al., 1998; O'Brien et al., 1998). Additional work on the chronology of deglacial events from the Antarctic margin, especially from the outer shelf (Pudsey et al., 1994, Pope and Anderson, 1992) is clearly needed to resolve this growing controversy.

Acknowledgements

The authors wish to thank participants and co-investigators on cruises of the USAP *Nathaniel B. Palmer* (NBP99-03 and NBP01-07), *L. M. Gould* (LMG98-02), JOIDES *Resolution* (ODP Leg 178), and the 2001 cruise of the R/V *Hesperides*. These efforts were supported by NSF Office of Polar Programs grants (OPP-9615053 and OPP-000306, to Hamilton College) the Joint Oceanographic Institutions (JOI/USSSP funding for ODP Leg 178), and the Spain-Italy-Belgium COHIMAR/SEDANO project (ref. REN2000-0896), Cooperación España - USA en investigación antártica en Geociencias Marinas (GEMARANT) (Ref. 99120, funded by the Spanish-USA Program for Scientific and Technological Cooperation) and Generalitat de Catalunya grant to CRG on Marine Geosciences of the University of Barcelona (Ref. 2001SGR 00076). Funding from Italy was through PNRA. Thanks are also extended to the Antarctic Marine Geology Facility, T. Janecek and his staff, at the Florida State University for their assistance with sediment cores.

References

- Alley, R.B., Dupont, T.K., Parizek, B.R., Anandakrishnan, S., Lawson, D.E., Larson, G.J., Evenson, E.B., 2004. Outburst flooding and surge initiation in response to climatic cooling: An hypothesis, this volume.
- Amblas, D., Urgeles, R., Canals, M., Rebesco, M., Estrada, F., Hugues-Clarke, J. E., and Calafat, A. M., The role of continental shelf glacial troughs in continental rise development off western North Antarctic Peninsula, *Quaternary Science Reviews* (in review).
- Anderson, J. B., 1999. *Antarctic Marine Geology*, Cambridge University Press, 289 pp.
- Anderson, J. B., Smith Wellner, J., Lowe, A. L., Mosola, A. B., and Shipp, S. S., 2001. Footprint of the expanded West Antarctic ice sheet: Ice stream history and behavior, *GSA Today* 11 (10), 4–9.
- Andrews, J. T., Domack E. W., Cunningham, W. L., Leventer, A., Licht, K. J., Jull, A. J. T., DeMaster, D. J., and Jennings, A., 1999. Problems and possible solutions concerning radiocarbon dating of surface marine sediments, *Antarctica, Quaternary Research*, 52, 206-216.

Barker, P. F., and Camerlenghi, A., 2002. Glacial history of the Antarctic Peninsula from Pacific margin sediments, In: Barker, P. F., Camerlenghi, A., Acton, G. D., and Ramsay, A. T. S. (Eds.), Proc. ODP, Sci. Results, 178 [CD ROM], College Station TX (Ocean Drilling Program), 1-40.

Barker, P. F., Camerlenghi, A., Acton, G. D. and others, 1999. Proc. Of the O.D.P. Initial Reports 178 [CD-ROM]. Available from: Ocean Drilling Program, Texas A&M Univ., College Station TX, 77845-9547, USA.

Bart, P. J., and Anderson, J. B., 1995. Seismic record of glacial events affecting the Pacific margin of the northwestern Antarctic Peninsula. In: Cooper, A.K., Barker, P.F., and Brancolini, G. (Eds.) Geology and Seismic Stratigraphy of the Antarctic Margin. Antarctic Research Series, 68, American Geophysical Union, Washington D. C, 75-95.

Benn, D. I., and Evans, D. J. A., 1998. Glaciers and Glaciation, Arnold, London, 734 pp.

Bentley, M. J., and Anderson, J. B., 1998. Glacial and marine geological evidence for the ice-sheet configuration in the Weddell Sea-Antarctic Peninsula region during the Last Glacial Maximum, Antarctic Science, 10, 309-325.

Björck, S., Hjort, C., Ingólfsson, Ó. and Skog, G., 1991. Radiocarbon dates from the Antarctic Peninsula region – problems and potential. In: Lowe J. J., (Ed.) Radiocarbon Dating: Recent Applications and Future Potential, Quaternary Proceedings No. 1, Quaternary Research Association, Cambridge, 55-6.

Bouma, A. H., 1987. Megaturbidite: an acceptable term? Geo-Marine Letters, 7, 63-67.

Brachfeld, S., Domack, E., Kissel, C., Laj, C., Leventer, A., Ishman, S., Gilbert, R., Camerlenghi, A., and Eglinton, L. B., 2003. Holocene history of the Larsen-A Ice Shelf constrained by geomagnetic paleointensity dating. Geology 31, 749-752.

Camerlenghi, A., Domack, E., Rebesco, M., Gilbert, R., Ishman, S., Leventer, A. Brachfeld, S. and Drake, A., 2001. Glacial morphology and post-glacial contourites in northern Prince Gustav Channel (NW Weddell Sea, Antarctica). Marine Geophysical Researches 22, 417-443.

Canals, M., Urgeles, R., and Calafat, A. M., 2000. Deep sea-floor evidence of past ice streams off the Antarctic Peninsula, Geology 28, 31-34.

Canals, M., Casamor, M.L., Urgeles, R., Calafat, A.M., Domack, E.W., Baraza, J., Farran, M., and DeBatist, M., 2002. Seafloor evidence of a subglacial sedimentary system off the northern Antarctic Peninsula. Geology 30, 603-606.

Canals, M., Calafat, A., Camerlenghi, A., DeBatist, M., Urgeles, R., Farran, M.L., Geletti, R., Versteeg, W., Amblàs, D., Rebesco, M., Casamor, J. L., Sánchez, A.,

Willmott, V., Lastras, G., Imbo, Y., 2003. Uncovering the footprint of former ice streams off Antarctica. *EOS* 84 (97), 102-103.

Clark, P. U., Mitrovica, J. X., Milne, G. A., Tamisiea, M. E., 2002. Sea-level fingerprinting as a direct test for the source of global meltwater pulse 1A. *Science* 295, 2438-2441.

Domack, E. W., 2002. A synthesis for Site 1098: Palmer Deep. In: Barker, P. F., Camerlenghi, A., Acton, G. D., and Ramsay, A. T. S., (Eds.), *Proc. ODP, Sci. Results, 178: College Station, TX (Ocean Drilling Program), Chapter 34, 1-14.*

Domack, E.W., and Williams, C.R., 1990. Fine-structure and suspended sediment transport in three Antarctic fjords. *Antarctic Research Series, American Geophysical Union* 50, 71-89.

Domack, E. W., Foss, D. J. P., Syvitski, J. P. M., and McClennen, C. E., 1994. Transport of suspended particulate matter in an Antarctic fjord. *Marine Geology* 121, 161-170.

Domack, E. W., O'Brien, P., Harris, P., Taylor, F., Quilty, P. G., DeSantis, L., and Raker, B., 1998. Late Quaternary sediment facies in Prydz Bay, East Antarctica and their relationship to glacial advance onto the continental shelf. *Antarctic Science* 10, 236-246.

Domack, E.W., Jacobson, E. A., Shipp, S.S., and Anderson, J.B., 1999. Late Pleistocene/Holocene retreat of the West Antarctic Ice Sheet in the Ross Sea: Part 2 – sedimentologic and stratigraphic signature, *Geological Society of America Bulletin* 111, 1517-1536.

Domack, E. W., Leventer, A., Dunbar, R. Taylor, F., Brachfeld, S., Sjunneskog, C. and ODP Leg 178 Scientific Party, 2001. Chronology of the Palmer Deep site, Antarctic Peninsula: a Holocene palaeoenvironmental reference for the circum-Antarctic. *The Holocene* 11, 1-9.

Domack, E.W., Leventer, A., Root, S., Ring, J., Williams, E., Carlson, D., Hirshorn, E., Wright, W., Gilbert, R., and Burr, G., 2003. Marine sedimentary record of natural environmental variability and recent warming in the Antarctic Peninsula. In: Domack, E.W., Leventer, A., Burnett, A., Bindschadler, R., Convey, P., and Kirby, M., (Eds.) *Antarctic Peninsula Climate Variability: A Historical and Paleoenvironmental Perspective, Antarctic Research Series, 79, American Geophysical Union, .*

Gilbert, R., Domack, E.W., and Camerlenghi, A., 2003. Deglacial history of the Greenpeace Trough: ice sheet to ice shelf transition in the northwestern Weddell Sea, In: Domack, E.W., Leventer, A., Burnett, A., Bindschadler, R., Convey, P., and Kirby, M., (Eds.), *Antarctic Peninsula Climate Variability: A Historical and Paleoenvironmental Perspective, Antarctic Research Series 79, American Geophysical Union, 195-204.*

Gjessing, J., 1960. Isavsmeltingstidens drenering, dens forløp og formdannende virkning i Nordre Atnedalen med sammenlignende studier fra Nordre Gudbrandsdalen og Nordre Østerdalen. *Ad Novas*, 3, Norw. geogr. Soc. Spec. Pub (492 pp).

- Gordon, J. E., and Harkness, D. D., 1992. Magnitude and geographic variation of the radiocarbon content in Antarctic marine life: implications for reservoir corrections in radiocarbon dating. *Quaternary Science Reviews* 11, 697-708.
- Harden, S. L., DeMaster, D. J., and Nittrouer, C. A., 1992. Developing sediment geochronologies for high-latitude continental shelf deposits: A radiochemical approach. *Marine Geology* 103, 69-97.
- Hawkes, D. D., 1981. Tectonic segmentation of the northern Antarctic Peninsula. *Geology* 9, 220-224.
- Hillefors, Å., 1979. Deglaciation models from the Swedish West Coast. *Boreas* 8, 153-169.
- Hjort, C., Ingólfsson, O., Bentley, M.J., and Björck, S., 2003. Late Pleistocene and Holocene glacial and climate history of the Antarctic Peninsula region: A brief overview of the land and lake sediment records. In: Domack, E.W., Leventer, A., Burnett, A., Bindschadler, R., Convey, P., and Kirby, M., (Eds.), *Antarctic Peninsula Climate Variability: A Historical and Paleoenvironmental Perspective*, Antarctic Research Series 79, American Geophysical Union.
- Ingólfsson, Ó., and Hjort, C., 2002. Glacial history of the Antarctic Peninsula since the Last Glacial Maximum—a synthesis. *Polar Research* 21, 227-234.
- Kapista, A. P., Ridley, J. K., de Q. Robin, G., Siegert, M. J., and Zotikov, I. A., 1996. A large deep freshwater lake beneath the ice of central East Antarctica, *Nature* 381, 684-686.
- Kirby, M.E., Domack, E.W., and McClennen, C.E., 1998. Magnetic stratigraphy and sedimentology of Holocene glacial marine deposits in the Palmer Deep, Bellingshausen Sea, Antarctica: implications for climate change? *Marine Geology* 152, 247-259.
- Larter, R. D., and Vanneste, L.E., 1995. Relict subglacial deltas on the Antarctic Peninsula outer shelf. *Geology* 23, 33-36.
- Larter, R.D., Rebesco, M., Vanneste, L.E., Gamboa, L.A.P., Barker, P.F., 1997. Cenozoic Tectonic, Sedimentary and Glacial History of the Continental Shelf West of Graham Land, Antarctic Peninsula. In: Cooper, A.K., Barker, P.F. (Eds.), *Geology and Seismic Stratigraphy of the Antarctic Margin II*. Am. Geophys. Union, Antarct. Res. Ser. 71, 1-27.
- Leventer, A., Domack, E., Barkoukis, A., McAndrews, B., and Murray, J., 2002. Laminations from the Palmer Deep: A diatom based interpretation, *Paleoceanography* 17, doi 10.1029/2001PA000624.

Lowe, A. L., and Anderson, J. B., 2002. Reconstruction of the West Antarctic ice sheet in Pine Island Bay during the Last Glacial Maximum and its subsequent retreat history. *Quaternary Science Reviews* 21, 1879-1897.

McMullen, K., Domack, E.W., Leventer, A., Dunbar, R., Brachfeld, S., 2002. Three stage ice sheet recession as recorded by swath bathymetry in the Mertz Trough: East Antarctica, *Eos Tran. AGU*, 83, C51A-9027.

O'Brien, P.E., DeSantis, L., Harris, P.T., Domack, E.W., and Quilty, P.G., 1998. Palaeo ice shelf grounding zones of western Prydz Bay, Antarctica – Sedimentary Processes from seismic and sidescan images. *Antarctic Science* 11, 78-91.

O'Cofaigh, C., Pudsey, C. J., Dowdeswell, J. A., and Morris, P., 2002. Evolution of subglacial beforms along a paleo-ice stream, Antarctic Peninsula continental shelf. *Geophysical Research Letters* 29, 10.1029/2001GL014488.

Ozward, G. K. A., and Robin, G. de Q., 1973. Lakes beneath the Antarctic Ice Sheet. *Nature* 245, 251-254.

Payne, A.J., Sugden, D.E., and Clapperton, C.M., 1989. Modeling the growth and decay of the Antarctic Peninsula Ice Sheet. *Quaternary Research* 31, 119-134.

Pope, P.G. and Anderson, J.B., 1992. Late Quaternary glacial history of the northern Antarctic Peninsula's western continental shelf: evidence from the marine record. *Antarctic Research Series* 57, American Geophysical Union, Washington DC, 63-91.

Pudsey, C.J., Barker, P.F., and Larter, R.D., 1994. Ice sheet retreat from the Antarctic Peninsula shelf. *Continental Shelf Research* 14, 1647-1675.

Rebesco, M., Camerlenghi, A., DeSantis, L., Domack, E.W., and Kirby, M., 1998. Seismic stratigraphy of Palmer Deep: a fault-bounded late Quaternary sediment trap on the inner continental shelf, Antarctic Peninsula margin. *Marine Geology* 151, 89-110.

Rebesco, M., Vedova, B.D., Cernobori, L., and Aloisi, G., 2000. Acoustic facies of Holocene megaturbidites in the Eastern Mediterranean. *Sedimentary Geology* 135, 65-74.

Shevenell, A., Domack, E.W., and Kernan, G.M., 1996. Record of Holocene palaeoclimate change along the Antarctic Peninsula: Evidence from glacial marine sediments, Lallemand Fjord. *Pap. Proc. R. Soc. Tas.* 130(2), 55-64.

Shipp, S., Anderson, J.B., and Domack, E.W., 1999. Late Pleistocene/Holocene retreat of the West Antarctic Ice-Sheet system in the Ross Sea: Part 1 – geophysical results, *Geological Society of America Bulletin* 111, 1486-1516.

Shipp, S., Wellner, J. S., Anderson, J. B., 2002. Retreat signature of a polar ice stream: sub-glacial geomorphic features and sediments from the Ross Sea, Antarctica, In:

Dowdeswell, J. A., and O’Cofaigh, C. (Eds.) Glacier-influenced Sedimentation on High-Latitude Continental Margins. Geological Society London, Special Publications 203, 277-304.

Shoemaker, E. M., 1991. On the formation of large sub-glacial lakes, Canadian Journal of Earth Sciences 28, 1975-1981.

Siegert, M. J., Dowdeswell, J. A., Gorman, M. R., and McIntyre, N. F., 1996. An inventory of Antarctic sub-glacial lakes. Antarctic Science 8, 281-286.

Skinner, B. J., Porter, S. C., and Botkin, D. B., 1999. The Blue Planet: An Introduction to Earth System Science. John Wiley, New York, 552 pp.

Smith, C. R. and Sandwell, D. T., 1997. Global seafloor topography from satellite altimetry and ship depth soundings. Science 277, 1956-1962.

Sniffen, P. J., 2001. Neotectonic development of the Palmer Deep, Antarctic Peninsula, BA Thesis, Hamilton College, Clinton New York, 37 pp.

Stuiver, M., Reimer, P., Bard, B., Beck, J.W., Burr, G.S., Hughen, K.A., Kromer, B., McCormack, Van Der Plicht, G. J., and Spurk, M., 1998. INTCAL98 radiocarbon age calibration, 24,000-0 cal. BP. Radiocarbon 40, 1041-1083.

Sugden D. E., and John, B. S. 1976. Glaciers and Landscape A Geomorphological Approach. John Wiley, New York, 376 pp.

Zwally, H. J., Abdalati, W., Herring, T., Larson, K., Saba, J., and Steffen, K., 2002, Surface melt-induced acceleration of Greenland Ice-Sheet flow. Science 297, 218-222.

Table 1: List of radiocarbon ages reported and incorporated in Fig. 10.

Lab # AA-	Core/Site ¹	mbsf ²	Total Organic Carbon %	$\delta^{13}\text{C}$	Uncorrected ¹⁴ C age ³	Calibrated age yr BP ⁴
29174	KC-26	0.005	1.01	-24.57	1610 \pm 55	modern
29175	KC-26	0.305	0.82	-24.83	2380 \pm 45	700 \pm 45
29176	KC-26	0.605	1.02	-24.14	2400 \pm 45	720 \pm 45
29177	KC-26	1.505	0.90	-24.88	3180 \pm 45	1520 \pm 45
29148	1099A	8.580	1.14	-24.58	4590 \pm 55	3250 \pm 55
29149	1099A	10.700	1.25	-23.67	4740 \pm 55	3400 \pm 55
29150	1099A	13.860	1.30	-23.40	5420 \pm 55	4290 \pm 55
29151	1099A	14.760	1.43	-23.57	5900 \pm 90	4870 \pm 90
29152	1099A	14.880	1.61	-23.06	6500 \pm 60	5640 \pm 60
29153	1099A	20.130	1.49	-23.11	6960 \pm 60	6170 \pm 60
29154	1099A	21.360	1.35	-22.64	7720 \pm 80	7000 \pm 80
29155	1099A	23.240	1.15	-23.43	8250 \pm 75	7540 \pm 75
29156	1099A	24.300	1.16	-23.49	8750 \pm 65	7970 \pm 65
29157	1099A	32.550	0.73	-24.24	9350 \pm 65	8590 \pm 65
29158	1099A	39.240	0.47	-25.02	12,680 \pm 80	12,990 \pm 80
29159	1099A	41.940	1.00	-24.84	9290 \pm 70	8530 \pm 70
29160	1099B	85.520	0.69	-23.17	11,300 \pm 90	11,090 \pm 90
29161	1099B	87.020	1.02	-22.85	11,760 \pm 70	11,650 \pm 70
29162	1099B	88.960	1.00	-23.38	9840 \pm 70	9030 \pm 70
29163	1099B	91.960	0.64	-24.14	10,945 \pm 70	10,330 \pm 70
29164	1099B	95.720	0.69	-24.77	10,890 \pm 70	10,317 \pm 70
29165	1099B	98.620	1.03	-23.22	10,990 \pm 70	10,570 \pm 70
29166	1099B	103.43	0.86	-23.04	11,830 \pm 75	11,880 \pm 75
29167	1099B	107.12	1.05	-22.73	12,120 \pm 80	12,580 \pm 80

AA = University of Arizona NSF-TAMS facility

¹Core KC-26 = kasten core 26 collected during cruise *LMG 98-02*, Sites are composite Holes 1099A and 1099B collected during ODP Leg 178.

²mbsf = depth in core below sea floor not adjusted for stratigraphic relationship and are given as mid-depths in 1 cm sample intervals.

³Uncorrected ages are rounded to the nearest 10 years and are adjusted for $\delta^{13}\text{C}$.

⁴Calibrated ages are derived via a surface correction for particulate reworking of 360 yrs, a reservoir correction of 1250 yrs (Björck et al., 1991), and the routine outlined by Stuiver et al., (1998).

List of Figures

Fig. 1. Swath bathymetry and GEOSAT seafloor bathymetry (depth in m) offshore Graham Land, western Antarctic Peninsula. Location of detailed Fig. 2 of Palmer Deep outlet system is indicated along with Anvers Island (AI), Biscoe Trough (BT), Bruce Plateau (BP) and Bismark Strait (BS). Lobes are inter-trough banks and drifts are sediment flows (after Barker and Camerlenghi, 2002). Reconstructed glacial flow lines are indicated by arrows with increasing width proportional to hierarchy of tributary systems. Insert shows location of study area in relation to Antarctica.

Fig. 2. Detailed shaded bathymetric map of the Palmer Deep region based upon Seabeam swath bathymetry (area of detail) stitched to coarse resolution bathymetry from GEOSAT data (Smith and Sandwell, 1997). Regions referred to in text include the PD basin (PD), Palmer Deep Outlet Sill (PDOS), and Hugo Island Trough (HIT), Joubin Islands (JI), Wauermans Islands (WI), Dannebrog Island (DI), Hugo Island (HI).

Fig. 3. Detail bathymetric contour (swath) map of the Palmer Deep region with a contour interval of 20 m. Location of ODP (Leg 178) Sites 1098 and 1099 indicated along with Jumbo Piston Core 10 (JPC-10, cruise *NBP* 99-03) and kasten cores 15-17 (cruise *NBP* 01-07).

Fig. 4. Outline map of major seafloor features of the Palmer Deep basin including the relict delta (inferred topsets and foresets), incised sediment gravity flow channel system, basin floor, debris flow slope, and terraces. See Fig. 3 for bathymetric details of outlined features.

Fig. 5. Seismic lines of across portions (color coded) of the Palmer Deep showing a smooth, steep depositional slope (yellow), a starved basin in the northeast (blue), and a rocky basement to the southwest (red) surrounding draping sediments (green). Vertical scale is two-way travel time in seconds.

Fig. 6. Gray scale swath bathymetry of the Palmer Deep Outlet Sill (PDOS), see Fig. 2 for regional location. Contour interval is 5 m.

Fig. 7. Outline map of major seafloor features of the PDOS and PD basin including gravity flow channels, relict delta, broad melt water channels, and dispersed melt water channels. Unidirectional arrows indicate uniform profiles that deepen into PD basin while bidirectional arrows indicate reversals in slope. Compare to Fig. 5 for bathymetric detail.

Fig. 8. Grey scale swath bathymetry of the Hugo Island Trough (HIT) showing locations of gravity cores collected during cruise *NBP*-01-07. See Fig. 2 for regional location. Contour interval is 10m.

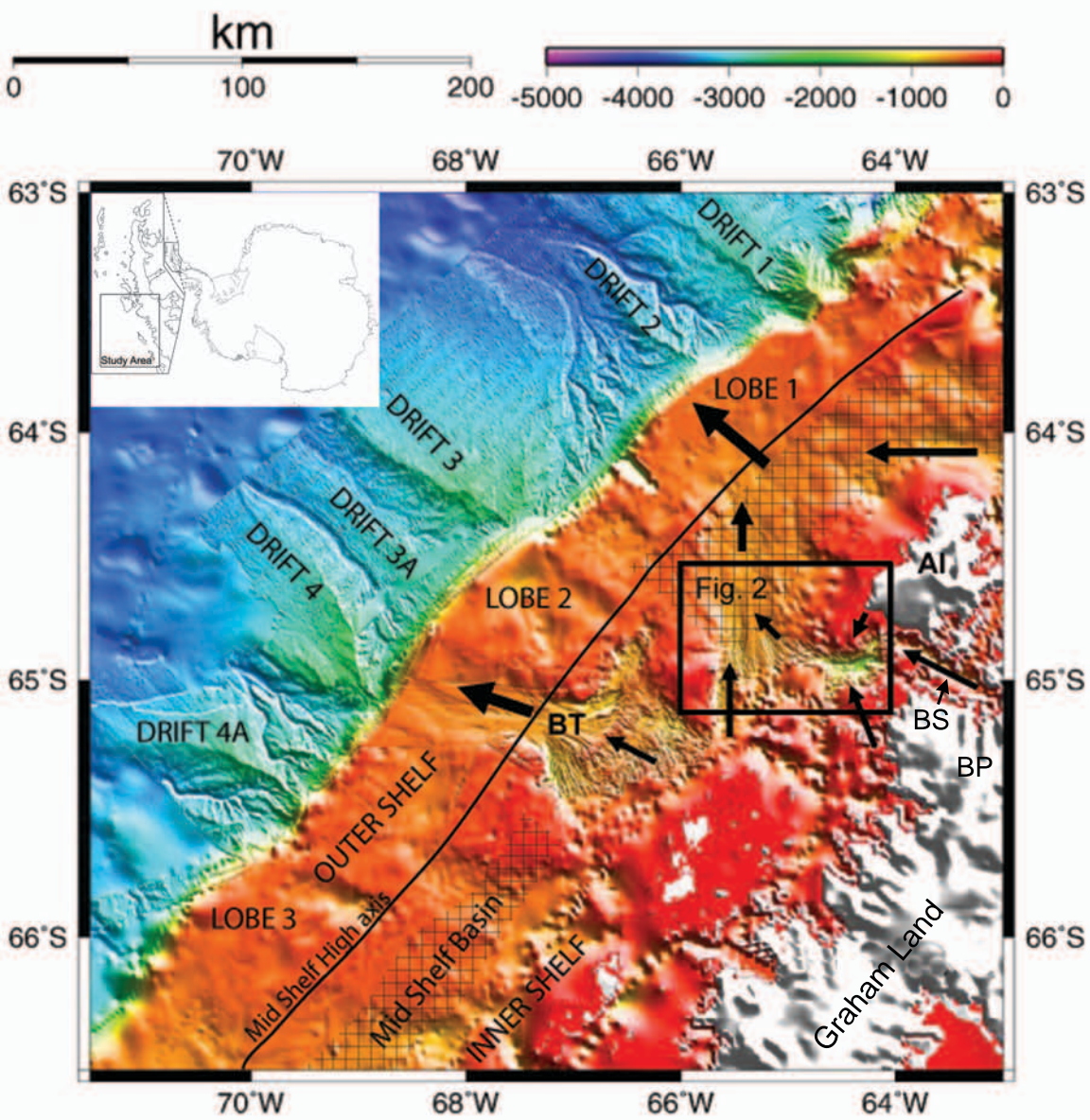
Fig. 9. Outline map of some of the seafloor features characteristic of the HIT region including mega-scale glacial lineations, drumlin forms, spindle-forms, and erosional

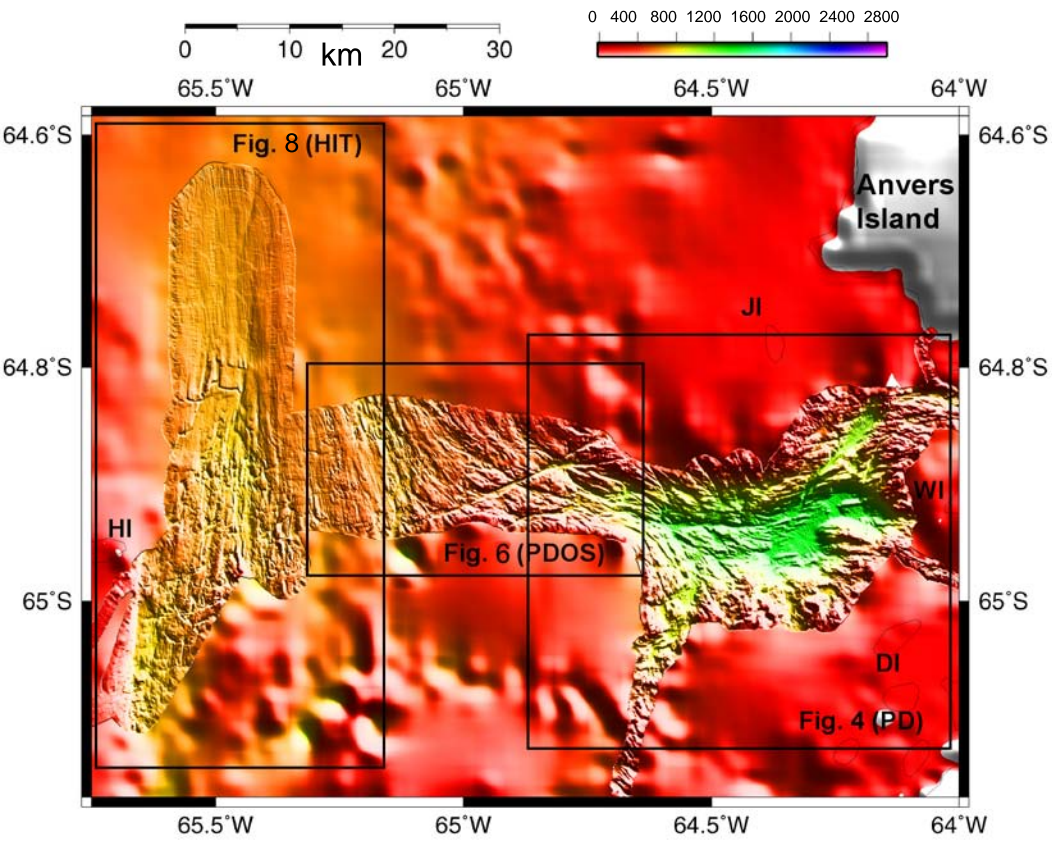
breaches of submarine ridges (a moraine or cuesta). On this later feature shading of negative (erosional) relief lies landward of positive (depositional) relief, thus suggesting the transfer of sediment via melt water through the breach point in a seaward direction following the ideas of McMullen et al., (2002). Compare to Fig. 7 for bathymetric detail.

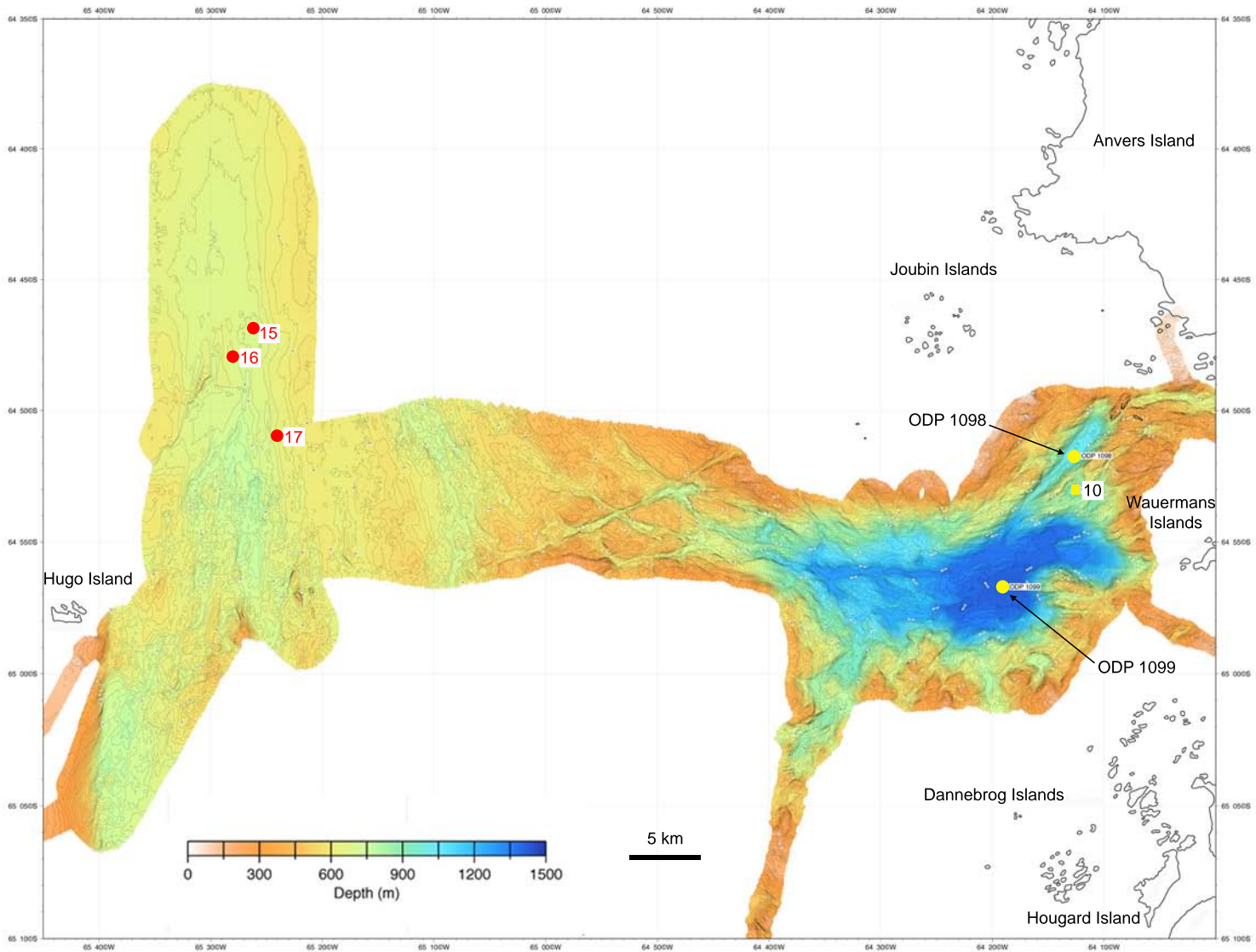
Fig. 10. Core lithology and radiocarbon chronology of cores from the PD basin along with magnetic susceptibility. All ages are listed in table 1, or are previously reported and discussed by Kirby et al., (1998) and Domack et al., (2001). Stratigraphic correlations between ODP Site 1099A,B and LMG98-2 core KC-26 are based upon physical correlation of key beds (turbidites) T1 through T6, recognized in other cores from the PD (Kirby et al., 1998). Correlations between 1099 and 1098 are based upon uncorrected radiocarbon ages (small font) that are corrected and calibrated (large font) as discussed in the text and in table 1. Calibrated ages for 1098 are listed as reported in Domack et al., (2001). MT refers to megaturbidite intervals and these along with Units I-IV are discussed in text.

Fig. 11. (a) View from over the Palmer Deep basin to the northeast of the elevated terrain of Anvers Island, with Mt Moberly and Mt. William to right of center, at elevations of 1524 m and 1506 m, respectively.
(b) View of one of the islands off the Graham Land Coast illustrating ice carapace and glacial/firn cover to sea level.
(c) View of Cape Renard (elevation of 743 m) along Graham/Danco Coast just southeast of Palmer Deep Basin illustrating erosional pinnacles indicative of radial flow patterns.

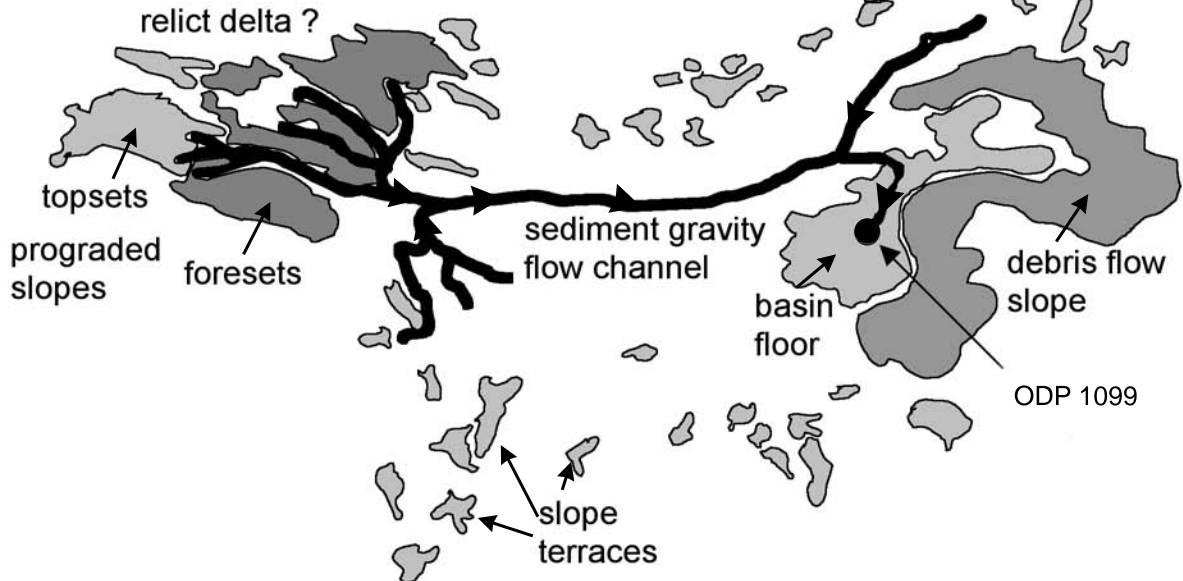
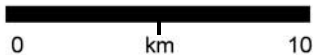
Fig. 12. (a) Regional outline map of PD ice stream (outlet) system and reconstructed grounding line position of Peninsula Ice Sheet during the LGM or MIS-2 (modified after Anderson, 1999). Ice flow directions are parallel, thin solid lines, ice domes by dotted lines, and drainage divides by bold dashed lines. Compare to Fig. 1 for relative scale. Note also the initiation of ice flow of the Gerlache Boyd Strait ice stream (Canals et al., 2000) at the divide with the PD system. Rectangle shows location of detailed flow in PD based upon Fig 2. The Biscoe Island system is outlined after Amblas et al., (in review).
(b) Cross-section along flow path of PD ice stream from the edge of the shelf (A) to the elevated spine of the Bruce Plateau (A'). Also shown is the hypothetical reconstruction of the surface profile of the PD system (dotted line), modern sea level, and the approximate sea level during maximum glaciation (dashed line). Note that there is no account of glacial isostatic adjustment of the crust in the reconstruction. Location of profile A-A' is in Fig. 12a. Location of ODP Leg 178 drilling sites are also shown.



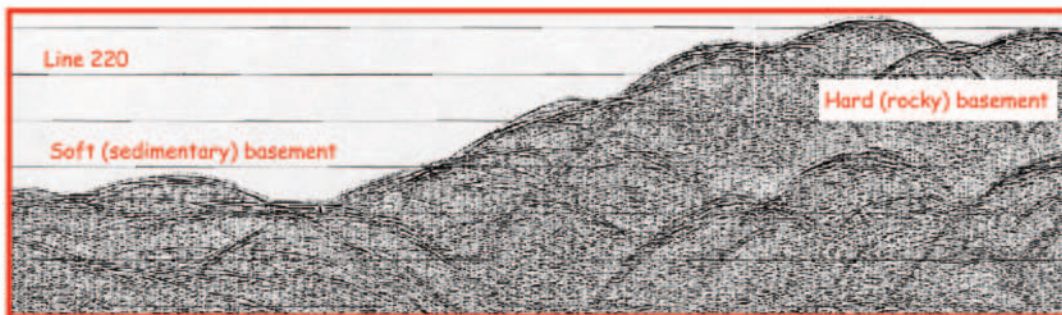
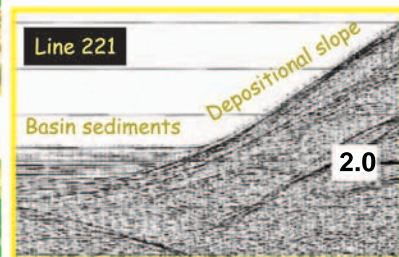
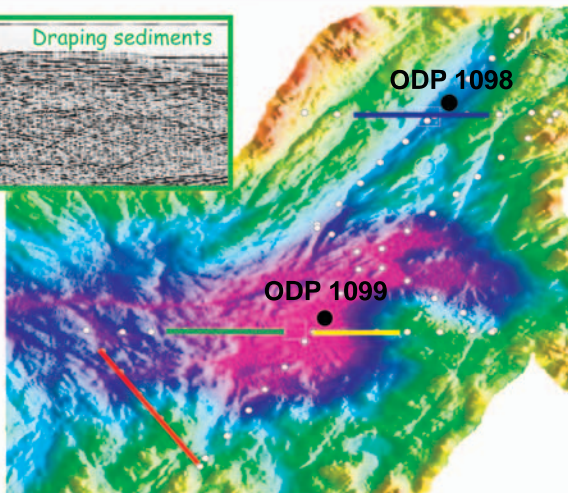
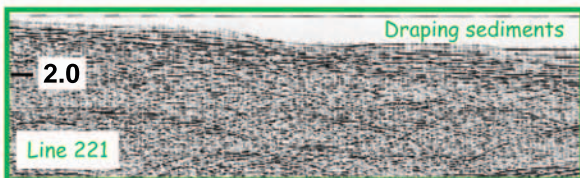
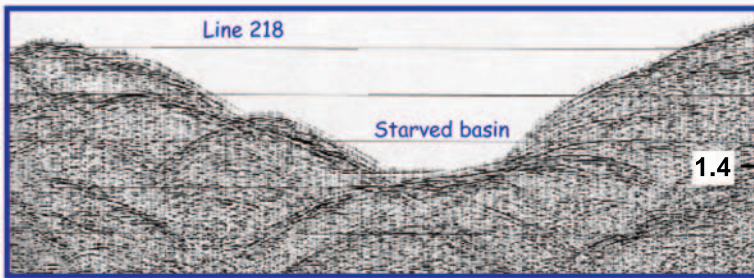


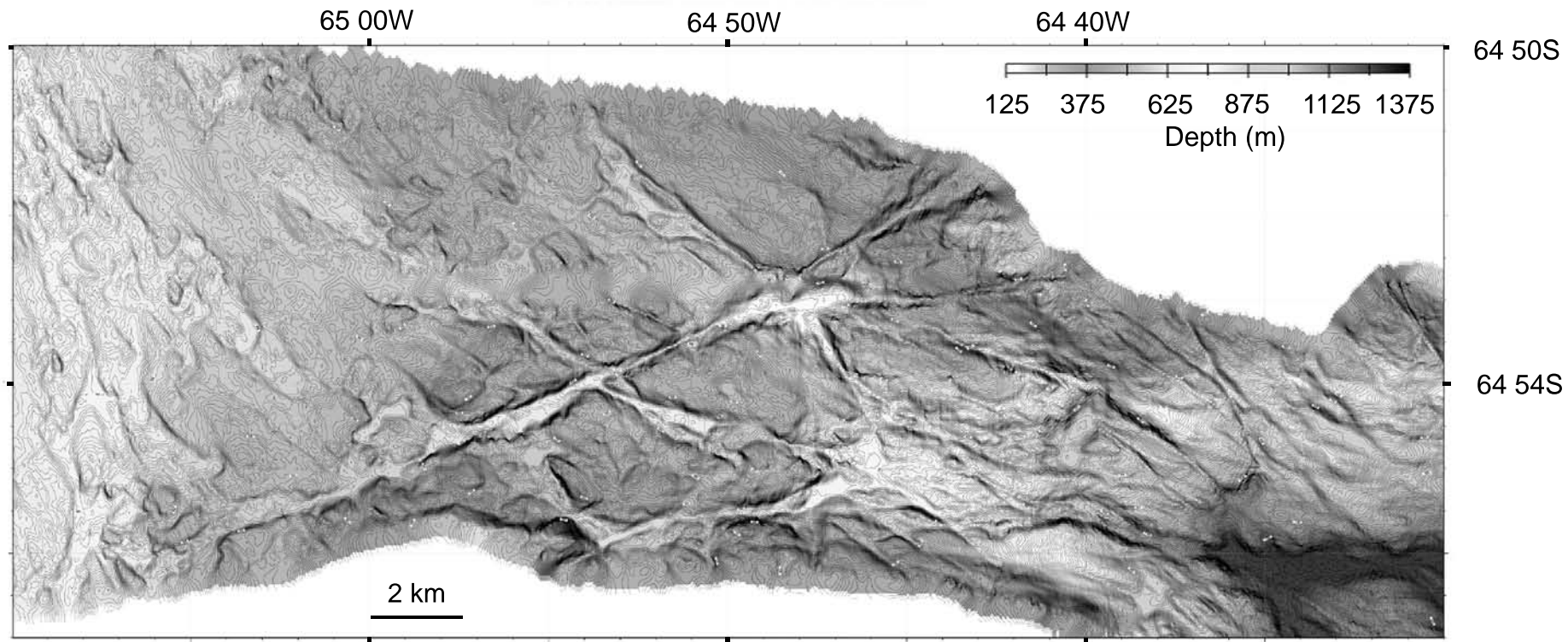


ODP 1098



ODP 1099

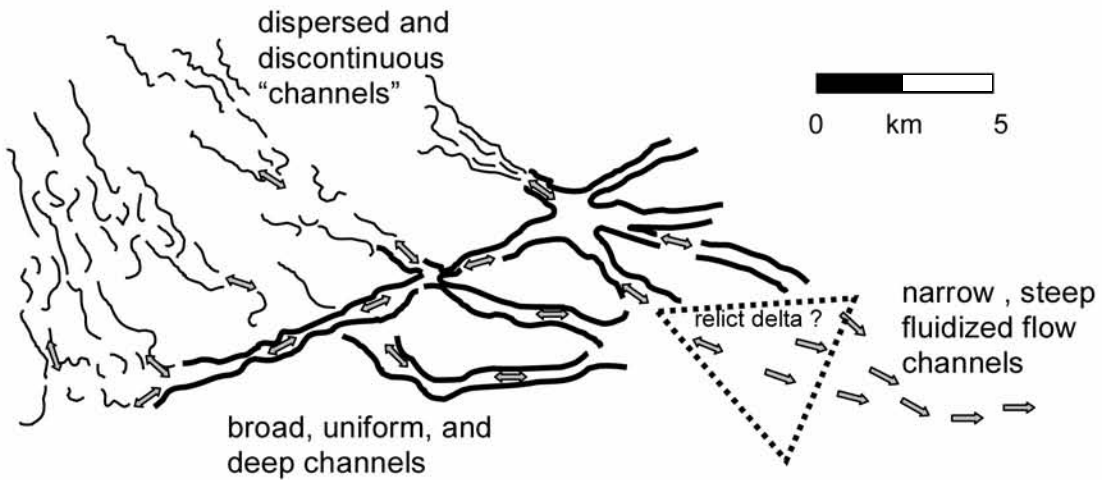




channels with change in slope direction



channels with uniform slope directions



dispersed and discontinuous "channels"

broad, uniform, and deep channels

0 km 5

narrow, steep fluidized flow channels

relict delta ?

65 40W

65 20W

64 40S

64 50S

65 00S

65 10S

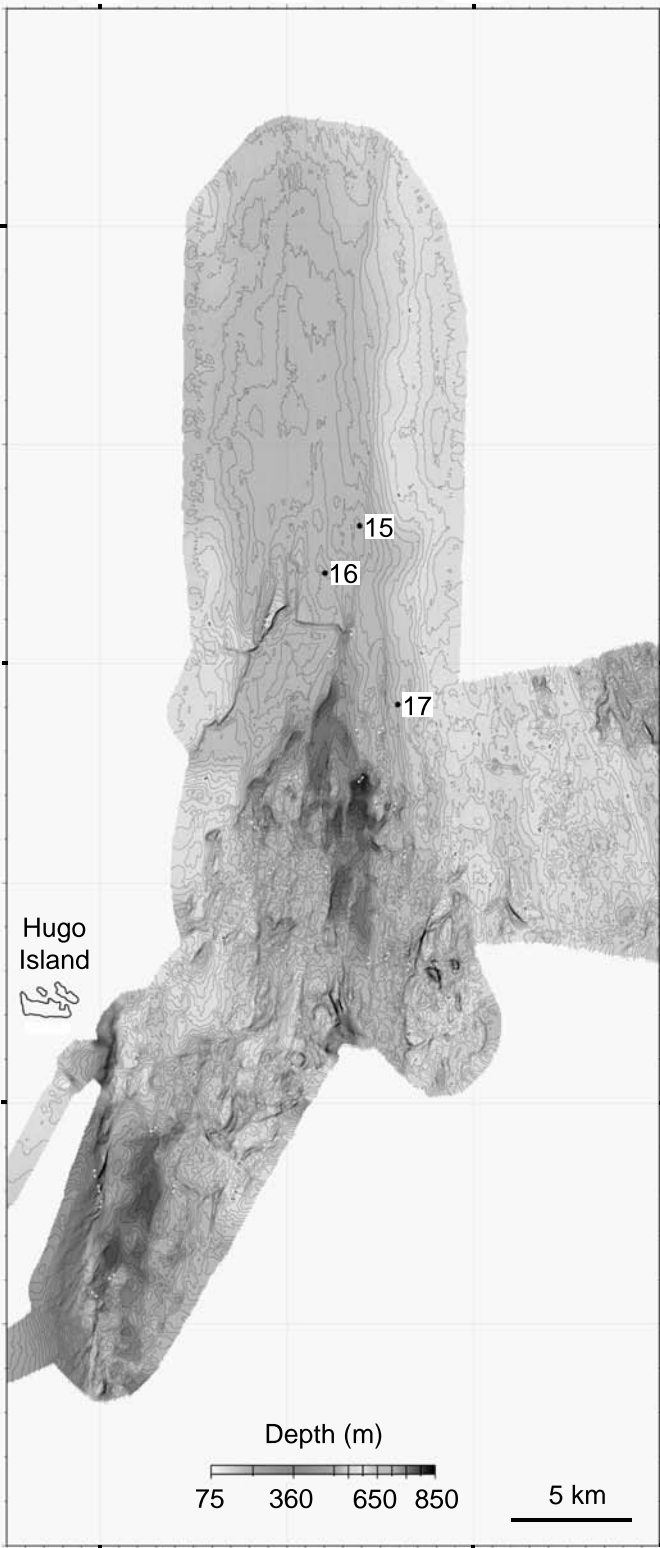
Hugo
Island



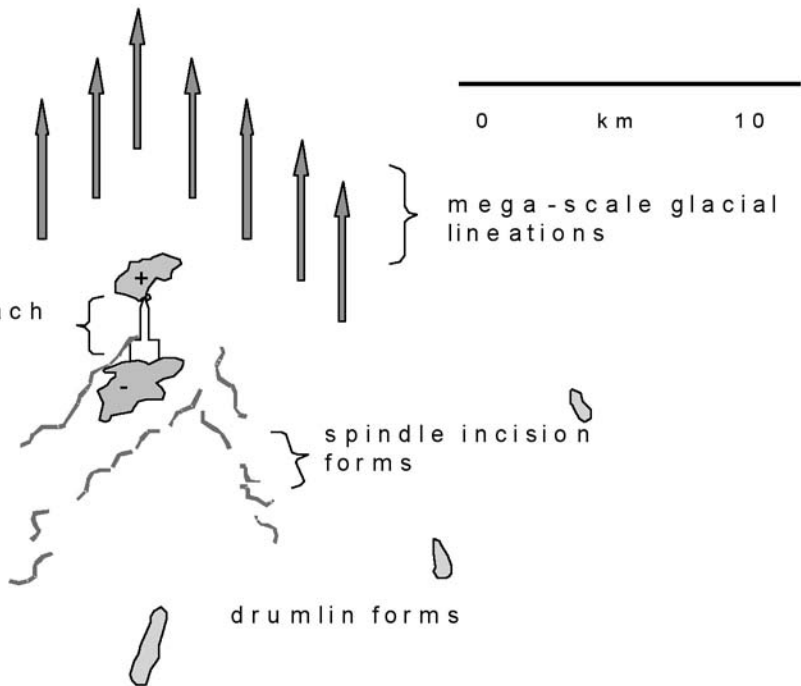
Depth (m)

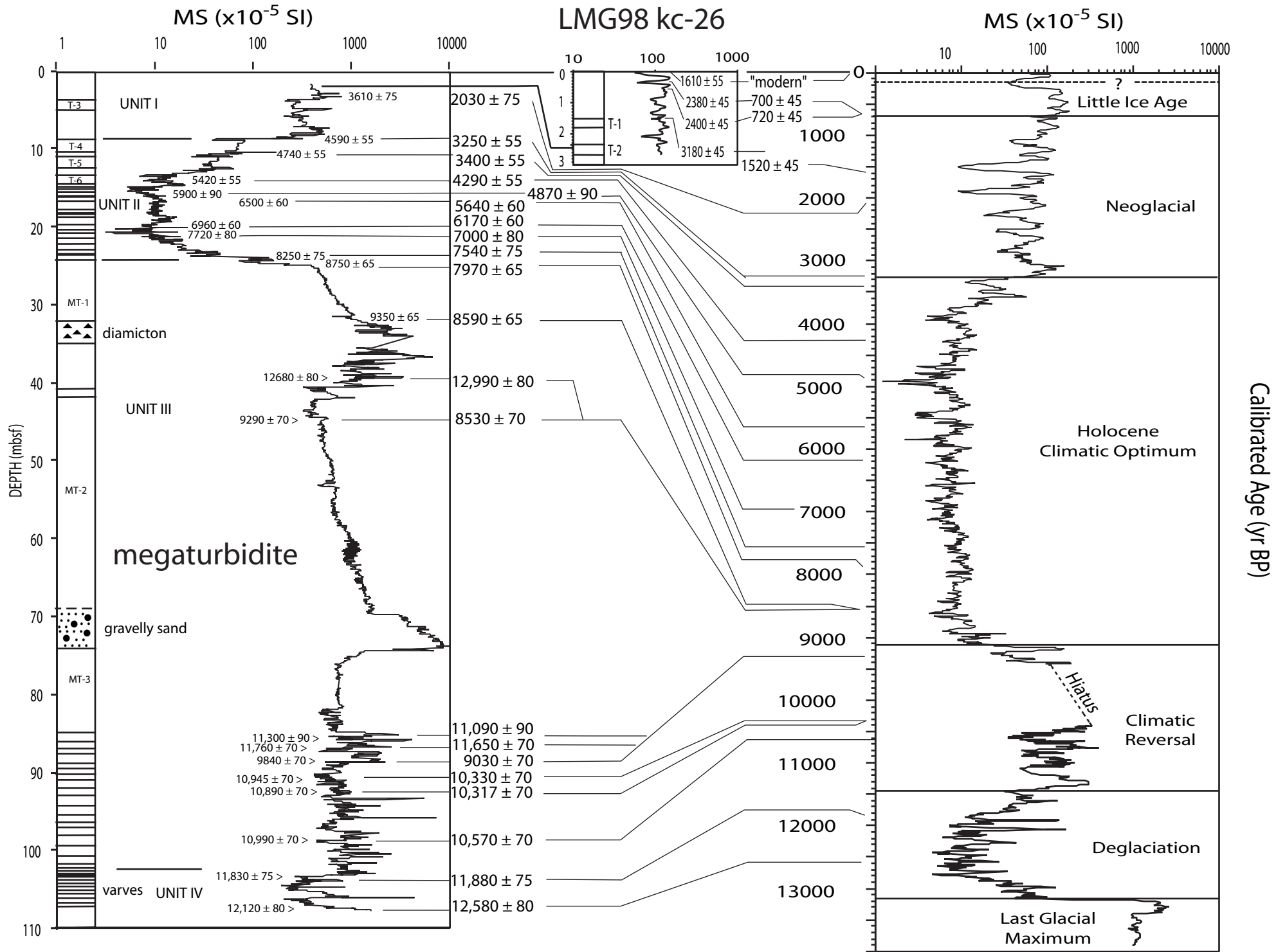
75 360 650 850

5 km



ridge breach
system

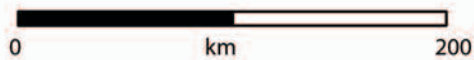




ODP Site :1099-A,-B

ODP Site: 1098-A,-B,-C





Bellingshausen Sea

